Carcinogenesis, 2019, 1–12

doi:10.1093/carcin/bgz178
Advance Access publication November 19, 2019
Original Article

ORIGINAL ARTICLE

A novel human colon signet-ring cell carcinoma organoid line: establishment, characterization and application

Yaqi Li[1,2,§], Renjie Wang[1,2,§], Dan Huang[2,3,§], Xiaoji Ma[1,2], Shaobo Mo[1,2], Qiang Guo[4], Guoxiang Fu[4], Yuanchuang Li[4], Xiaoya Xu[4], Xiang Hu[1,2], Yi Zhou[4], Yun Deng[5], Long Zhang[1,6], Honghong Chen[4], Jianjun Gao[4], Zhen Zhang[5], Sanjun Cai[1,2,†], Guoqiang Hua[4,6,†] and Junjie Peng[1,2,†,*]

[1]Department of Colorectal Surgery, Fudan University Shanghai Cancer Center, Shanghai 200032, China; [2]Department of Oncology, Shanghai Medical College, Fudan University, Shanghai 200032, China; [3]Department of Pathology, Fudan University Shanghai Cancer Center, Shanghai 200032, China; [4]Institute of Radiation Medicine, Fudan University, Shanghai 200032, China; [5]Department of Radiation Oncology, Fudan University Shanghai Cancer Center, Shanghai 230032, China; and [6]Cancer Institute, Shanghai Cancer Center, Fudan University, Shanghai, 230032, China

[§]Yaqi Li, Renjie Wang, and Dan Huang contributed equally to this work.
[†]These authors jointly supervised this work.
[*]To whom correspondence should be addressed. Fudan University Shanghai Cancer Center, 270 Dong'an Road, Xuhui, Shanghai 200032, China. Tel/Fax: +86 021 64175590; Email: pengjj67@hotmail.com
Correspondence may also be addressed to Guoqiang Hua, Institute of Radiation Medicine, Fudan University, 2094 Xie-Tu Road, Shanghai 200032, China. Tel/Fax: +86 21 64436705; Email: guoqianghua@fudan.edu.cn
Correspondence may also be addressed to Sanjun Cai, Fudan University Shanghai Cancer Center, 270 Dong'an Road, Xuhui, Shanghai 200032, China. Tel/Fax: +86 021 64175590; Email: caisanjuncsj@163.com

Abstract

Colon signet-ring cell carcinoma (SRCC) is a rare type of malignant dedifferentiated adenocarcinomas, and is associated with poor survival. However, an in-depth study of the biological features of SRCC is hindered by the lack of a reliable *in vitro* model of colon SRCC. Thus, the establishment of cell cultures from SRCC has become the most challenging task. Here, by harnessing the power of the organoid culture system, we describe the establishment of a human colon SRCC organoid line from a surgical sample from one patient with colon SRCC. The colon SRCC organoid line, YQ-173, was characterized for morphology, histology, ultrastructure and chromosome stability levels, showing that it resembles the histological and growth characteristics of the original tumor cells; xenografts were used to show that it also has a high tumor formation rate. RNA sequencing of YQ-173 compared with the normal tissue verified its mucinous nature. Capture-based targeted DNA sequencing combined with drug screening based on a bespoke 88 compound library identified that JAK2 might be a treatment target. An *in vitro* drug screening found that AT9283 and Pacritinib could be effective JAK2 inhibitors, which was consistent with the *in vivo* xenograft response. We report, for the first time, the establishment of an SRCC organoid line allowing in-depth study of SRCC biology, as well as a strategy to assess *in vitro* drug testing in a personalized fashion.

Received: 11 May 2019; **Revised:** 9 October 2019; **Accepted:** 19 October 2019

Abbreviations

3D	three-dimensional
DMEM	Dulbecco's modified Eagle's medium
ECM	extracellular matri
ENR	epidermal growth factor–Noggin–Rspondin
EpCAM	epithelial cell adhesion molecule
ERBB3	erb-b2 receptor tyrosine kinase 3
FBS	fetal bovine serum
HISC	human intestinal stem cell
IHC	immunohistochemistry
IF	immunofluorescence
JAK/STAT	Janus kinase/signal transducers and activators of transcription
KEGG	Kyoto Encyclopedia of Genes and Genomes
KRAS	Kirsten rat sarcoma viral oncogene homolog
LOESS	locally weighted regression
MET	mesenchymal to epithelial transition factor
MLH1	mutL homolog 1
MSH2	mutS homolog 2
RNAseq	RNA-sequencing
RTK/RAS	receptor tyrosine kinase (RTK)/Ras
SMAD4	SMAD family member 4
SRCC	signet-ring cell carcinoma
TNM	Tumor/Node/Metastasis

Introduction

Signet-ring cell carcinoma (SRCC) is a rare type of malignant dedifferentiated adenocarcinomas, which is defined as the presence of more than 50% of signet-ring cells by the World Health Organization (1). Signet-ring cells exhibit round shapes with eccentric nuclei and have abundant intracytoplasmic mucus granules. Only approximately 1% of colorectal cancers are SRCCs (2–4), but late diagnosis at more advanced tumor stages, observed high risk local recurrence and limited benefit from chemoradiotherapy make SRCCs of great clinical research value (5). Contradictory to the compelling need for deep study of colorectal SRCC, there are few available research tools due to its rarity. The establishment of an *in vitro* model is expected to one of the most desirable approaches to elucidate the biological features of SRCC.

Organoids are three-dimensional (3D) structures grown from stem cells that consist of organ-specific cell types (6). Organoids retain the structure, morphology, genetic mutations and heterogeneity of the parental tumor, and are now widely used to model different cancers, including those of the colon, stomach, lung, pancreas, liver, breast, prostate and fallopian tube (7). Adopting a 3D patient-derived organoid culture system, high-throughput drug screening coupled with genomic analysis offers individual patients, especially for patients with rare tumors, a unique opportunity to identify effective cancer therapies.

To our best knowledge, there are no reports on the *in vitro* or *in vivo* research model of colon SRCC. Here, we report the first establishment and characterization of a colon signet-ring carcinoma organoid line based on an organoid culture system derived from the primary tumor of a 43-year-old female patient with signet ring cell colon carcinoma with metastases to bilateral ovaries. The organoid line has been characterized for morphology, histology, chromosome stability, gene mutation and expression profile levels. Our data showed that the colon SRCC organoid line recaptures characteristics of the original tumor cells, and the SRCC organoid model can be used for *in vitro* drug screenings that are consistent with the *in vivo* xenotransplantation response.

Materials and methods

Patient

The organoid was derived from the primary tumor from a 43-year-old Chinese female patient who had colon cancer with metastases to bilateral ovaries. The histopathological diagnosis from endoscopic resection of bilateral ovaries was confirmed as metastatic SRCC. Radical resection of the primary tumor was performed in October 2016. The pathological report indicated that the primary tumor was a poorly differentiated colon SRCC, infiltrating to subserosa, without metastatic lymph node or venous/perineural invasion, and that the pathological Tumor/Node/Metastasis stage was pT4aN0M1. The patient completed eight cycles of FOLFOX regimens and has been under intensive surveillance. The patient was last followed-up on 15 March 2018 and no signs of recurrence or metastasis were discovered. The tissue was obtained with informed consent, and this study was approved by the ethical committee of Fudan University Shanghai Cancer Center.

Establishment of the patient-derived organoid

The isolation of tumor cell aggregates was performed essentially as described by Sato *et al* (8). Tumors were minced and portions were processed for histology assessment and DNA isolation. The remainder was cut into smaller pieces, washed three times with cold phosphate-buffered saline (PBS) with penicillin/streptomycin and incubated in digestion buffer (Supplementary Table 1, available at *Carcinogenesis* Online) for 30 min at 37°C in a water bath while shaking. Tubes were then shaken vigorously to isolate crypts and cell aggregates. Isolated crypts and cells aggregates were then embedded in Matrigel (Corning, 356231) on ice and seeded in 24-well plates (200 crypt-like structures per 50 µl of Matrigel per well). The Matrigel was polymerized for 5 min at 37°C, and 500 µl/well culture medium was overlaid. The cells were incubated at 37°C and 5% CO_2, and the culture medium was refreshed every 2 days.

Four different culture media were compared for the selection of the optimal culture medium for SRCC including Dulbecco's modified Eagle's medium plus 10% fetal bovine serum (FBS), Advanced DMEM-F12 plus 10% FBS, human intestinal stem cell (HIEC) medium minus Wnt-3A and epidermal growth factor–Noggin–Rspondin (ENR) plus 10% FBS. Five factors, SB202190, Gastrin, PGE2, A83-01 and NICO, were diluted in HIEC medium and added separately into the selected medium to detect their function on SRCC growth. Reagents and concentrations of each growth factor in different media are indicated in Supplementary Table 1, available at *Carcinogenesis* Online. Cancer cells (1×10^4) were seeded in 50 µl of Matrigel in 24-well plate overlaid with different mediums and cultured for 10 days. The number of organoids was counted every other day under a phase-contrast microscope. After culturing for 2 weeks, cell aggregates containing signet-ring cells became robust and lively in the optimized medium, while other crypts and cells died. Thus, the resulting aggregates were passaged routinely at a split ratio of 1:5 or 1:10. The SRCC organoid line was successfully established and named YQ-173.

Transfer from 3D to two-dimensional (2D) culture of YQ-173

3D-cultured YQ-173 organoids were prepared with the same protocol used for passaging, collected in 2D medium (ENR plus 10% FBS, Supplementary Table 1, available at *Carcinogenesis* Online) and seeded in flasks. Cultures were kept at 37°C and 5% CO_2 in a humidified incubator. The 2D-cultured YQ-173 cells were deposited at the China Center for Typical Culture Collection with the access number C2017222. YQ-173 organoids were used for histology assessment, immunohistochemistry (IHC) staining, immunofluorescence (IF) staining, quantitative real-time PCR (qRT-PCR), RNA and DNA sequencing, and drug screening. The 2D-cultured cells (banked before Passage 10) were used for electron microscopy study, chromosome analysis and xenografts (Supplementary Figure 1, available at *Carcinogenesis* Online).

Colorectal cancer cell culture

Human colon cancer cell lines (RKO, Caco-2 and LoVo) were originally purchased from American Type Culture Collection (Manassas, VA) and were used in our laboratory within 6 months. RKO, Caco-2 and LoVo were maintained in Dulbecco's modified Eagle's medium (Life Technologies, 31966) supplemented with 10% FBS. The normal colon mucosa cell line NCM460 was used as control and was maintained in Roswell Park Memorial Institute 1640 Medium (Life Technologies, 11875) supplemented with 10% FBS. All cell lines were cultured in a humidified atmosphere of 5% CO_2 at 37°C.

Histology assessment

Tissue samples or gels with organoids were washed with PBS, fixed in freshly prepared 4% neutral buffered paraformaldehyde (9) and embedded in paraffin blocks. Hematoxylin and eosin staining was performed as described (10) for morphological observation.

IHC staining

Formalin-fixed tissues or gels with organoids were cut into 4 μm sections and placed on polylysine-coated slides. Paraffin sections were baked for 1 h at 56°C, deparaffinized in xylene, rehydrated through graded ethanol, processed for antigen retrieval by pan heating in citrate (pH = 6.0) or ethylenediaminetetraacetic acid (pH = 9.0) antigen retrieval solution and quenched for endogenous peroxidase activity in 0.3% hydrogen peroxide for 10 min. Sections were then blocked for 1 h with 10% goat serum in 0.1% PBST and incubated with primary antibody overnight at 4°C. Primary antibodies for immunohistochemistry were mouse anti-Ki-67 (BD Pharmingen, Clone B56, 550609; dilution 1:500), mouse anti-β-catenin (BD Transduction Laboratories, Clone 14, 610153; dilution 1:100), rabbit anti-OLFM4 (CST, Clone D1E4M, 14369; dilution 1:200) and c-myc (Abcam, Clone Y69, ab32072; dilution 1:200). Immunostaining was performed using EnVision+System-HRP (AEC) (Dako, K4005). Subsequently, sections were counterstained with hematoxylin (Sigma) and mounted in a non-aqueous mounting medium.

IF staining

For IF staining, paraffin sections were baked for 1 h at 56°C, deparaffinized in xylene, rehydrated through graded ethanol and processed for antigen retrieval by pan heating in citrate (pH = 6.0) antigen retrieval solution. Sections were then blocked for 1 h with 10% donkey serum in 0.1% PBST and incubated with primary antibody overnight at 4°C. Primary antibodies for IF were rabbit anti-Mucin 2 (Santa Cruz, clone H-300, sc-15334; dilution 1:200) and polyclonal goat anti-EpCAM (R&D, AF960; dilution: 1:400). Slides were incubated with secondary antibodies of Tyramide Alexa Fluor 488 (Invitrogen, T20932, dilution 1:200) and Tyramide Alexa Fluor 594 (Invitrogen, T20935, dilution 1:200) for 2 h at room temperature. Slides were counterstained with 4′,6-diamidino-2-phenylindole (Sigma Aldrich, D9542, 5 μg/ml) for 10 min and mounted. Multichannel fluorescence images were acquired using an upright widefield Zeiss Aixo2 M2 imaging microscope with an Axiocam 506 color camera.

RNA isolation and qRT-PCR

RNA of cell lines, organoids and tissue samples was extracted using RNeasy mini kit (QIAGEN, 74104) according to the manufacturer procedures and the protocol. A PrimeScript™ RT Master Mix (Perfect Real Time) kit (Takara, RR036A) was used to produce cDNA. qRT-PCR was performed in ABI 7900HT (Applied Biosystems) using SYBR *Premix Ex Taq* II (Tli RNaseH Plus) kit (Takara, RR820A). RNA expression was normalized to *GAPDH*. Primers for *GAPDH* (F: 5′-GCACCGTCAAGGCTGAGAAC-3′; R: 5′-TGGTGAAGACGCCAGTGGA-3′), *MUC2* (F: 5′-CAAGATCTTCATGGG GAGGA-3′; R: 5′-AACACGGTGGTCCTCTTGTC-3′) and *TFF3* (F: 5′-CTCC AGCTCTGCTGAGGAGT-3′; R: 5′-GCTTGAAACACCAAGGCACT-3′) were used. All reactions were run in triplicate.

Electron microscopy

The 2D-cultured YQ-173 cells were centrifuged, washed in cold PBS and fixed overnight with 2.5% glutaraldehyde at 4°C. The cells were then fixed using 1% osmium tetroxide, followed by dehydration with an increasing concentration gradient of ethanol and propylene oxide. The sample was then embedded, cut into 50-nm sections and stained with 3% uranyl acetate and lead citrate. Images were acquired using a JEM-1200 electron microscope (JEOL, Tokyo, Japan)

Chromosome analysis

Chromosome analysis of YQ-173 cells was performed as described previously (11). The 2D-cultured cells were treated with colcemid at a concentration of 10 μg/ml for 3 h. The cells in metaphase were then harvested, treated with 75 mM hypotonic KCl for 20 min at 37°C and fixed in methanol and acetic acid (3:1). In a humidified environment, the cells were dropped onto a glass slide and stained with Giemsa solution. The metaphase chromosomes were observed under a microscope.

RNA-sequencing (RNA-seq) analysis

RNA-seq libraries were prepared using a VAHTS™ mRNA-seq V3 Library Prep Kit for Illumina® (Vazyme) following the manufacturer's instructions. Sequencing reads from RNA-seq data were aligned using the spliced read aligner HISAT2, which was supplied with the Ensembl human genome assembly (Genome Reference Consortium GRCh38) as the reference genome. Gene expression levels were calculated by the fragments per kilobase of transcript per million mapped reads. Annotations for the mRNA in the human genome were retrieved from the GENCODE (v25) database. The significant candidates were extracted with fold change (median) >2 or <0.5 and *P* value <0.05. The significantly differentially expressed genes were tested for Kyoto Encyclopedia of Genes and Genomes (KEGG) pathway enrichment using the Database for Annotation, Visualization and Integrated Discovery v6.8. The enriched pathways were filtered with a *P* value <0.01. Gene Set Enrichment Analysis was used to investigate the enrichment of cancer hallmark signatures from MSigDB 5.0.

DNA isolation and capture-based targeted DNA sequencing

Genomic DNA was extracted using a QIAamp DNA mini kit (QIAGEN, 51304) according to the manufacturer's procedures. Genetic profiles of all samples were assessed by performing capture-based targeted deep sequencing using the OncoScreen panel (Burning Rock Biotech Ltd), covering 2.02 MB of human genomic regions, including all exons and critical introns of 295 genes (Supplementary Table 2, available at *Carcinogenesis* Online). DNA quality and size were assessed by a high sensitivity DNA assay using a bioanalyzer. All indexed samples were sequenced on a NextSeq 500 (Illumina) with pair-end reads. The sequencing data in the FASTQ format were mapped to the human genome (hg19) using BWA aligner 0.7.10. Local alignment optimization, variant calling and annotation were performed using GATK 3.2, MuTect and VarScan, respectively. DNA translocation analysis was performed using both Tophat2 and Factera 1.4.3. Gene-level copy-number variation was assessed using a t statistic after normalizing read depth at each region by total read number and region size, and correcting GC-bias using a locally weighted regression algorithm.

Drug screening

YQ-173 organoids were harvested, mechanically split and diluted to 1×10^5 cells/ml in Matrigel. A 10 μl cell suspension was added to 96-well plates (Corning) and allowed to grow for 3 days. Eighty-eight drugs (Selleckchem, Supplementary Table 5, available at *Carcinogenesis* Online) at a concentration of 10 μM diluted in growth medium as well as dimethyl sulfoxide controls were then added in duplicate. The viability of organoids was measured after 3 days using the Cell Counting Kit-8 (Dojindo).

Selected drugs were then further validated *in vitro*. YQ173 organoids were split and diluted to 1×10^6 cells/ml in Matrigel. A total of 15 μl cell suspension seeded to 48-well plates (Corning) and allowed to grow for 3 days. Then, six concentrations of selected drugs, AT9283 and Pacritinib, as well as 5-FU (Selleckchem, S1209), and CPT11 (Selleckchem, S2217) were added in duplicate. The viability of organoids was measured after 5 days using the Cell Counting Kit-8 5 days. The data were analyzed using GraphPad Prism 6 followed by manual determination of half-maximal inhibitory concentration (IC_{50}) values.

Transplantation into athymic BALB/c nude mice

To test the *in vivo* tumorigenesis of established YQ-173 cells, xenotransplantation (5×10^6 cells/50 µl PBS with 50 µl Matrigel) was performed using male athymic BALB/c nude mice (n = 5, 6–8 weeks of age, Shanghai SLAC Laboratory Animal Co., Ltd). Tumor size was measured every other day with calipers from the time of the formation of palpable tumors. Tumor volume was calculated by the formula of length × width^2 × 0.5 (12). Six weeks after implantation, the mice were killed, and the tumors were removed and fixed for histological and IF staining.

To validate the effect of AT9283 *in vivo*, mice with established tumors (average volume of approx. 100 mm^3) were randomly divided into two groups (6 mice/group) and treated with vehicle or AT9283 (20 mg/kg, i.p. qd, 5 days on, 2 days off) for 3 weeks. For *in vivo* dosing, AT9283 was dissolved

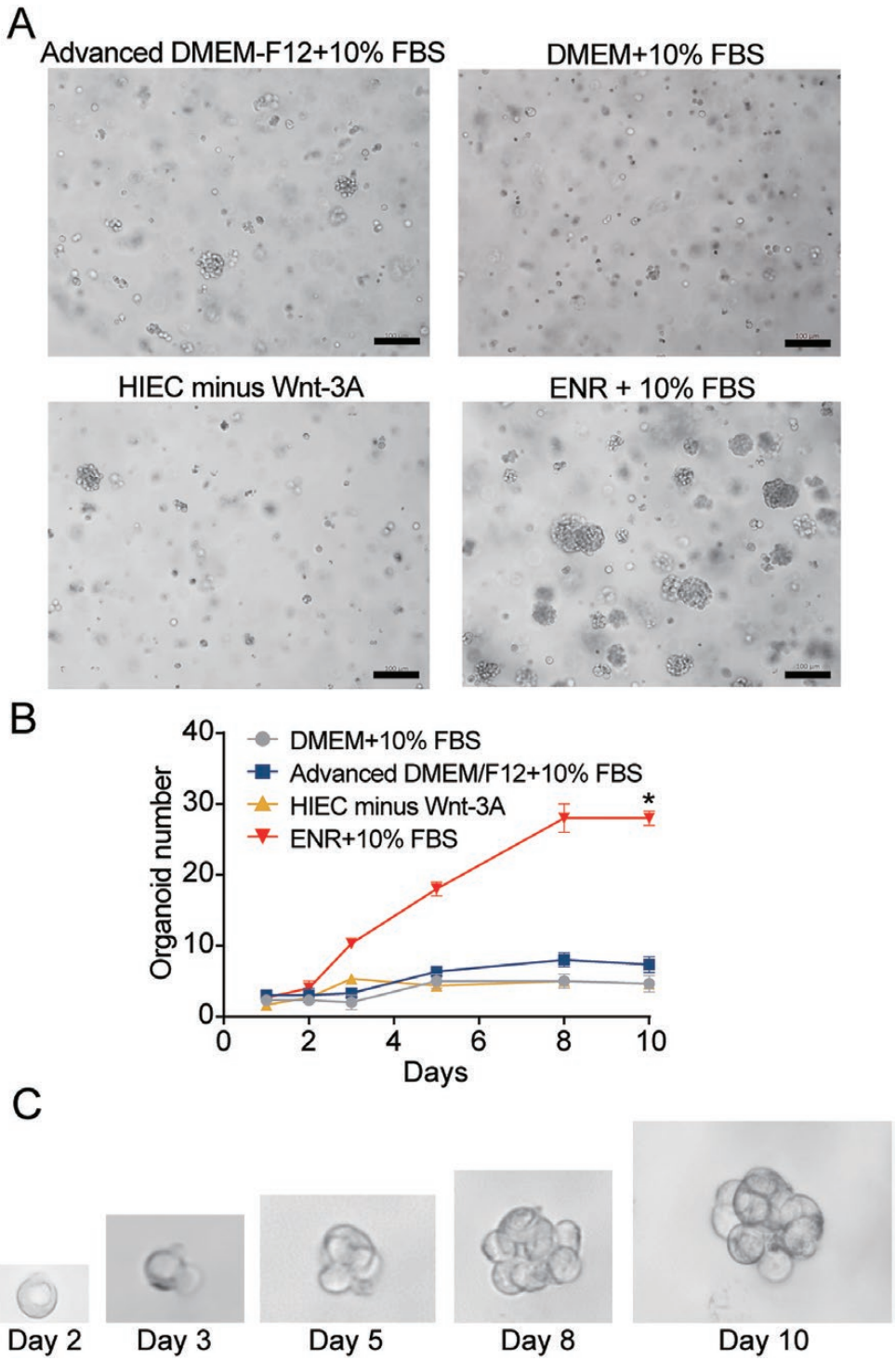

Figure 1. Optimal of culture medium and growth pattern of the colon signet-ring cell carcinoma organoids. (A) Representative images of organoids after culturing for 8 days in different culture media. Scale bar, 100 µm. (B) Comparison of organoid number per field during culture in different culture media. *$P < 0.05$. Two-way analysis of variance. Error bars indicate SEM. n = 3. (C) Time course culture of the colon signet-ring cell carcinoma organoids. Abbreviation: DMEM, Dulbecco' s modified Eagle medium; FBS, fetal bovine serum; HISC medium, human intestinal stem cell medium; ENR medium, epidermal growth factor–Noggin–Rspondin medium.

in 2% dimethyl sulfoxide, 30% PEG 300 (Sigma, 202371) and ddH_2O. Tumor size and mouse weight were determined three times a week. Animals were killed with CO_2 before the tumors reached a volume of 1500 mm^3. All animal experiments were performed according to the guidelines for the care and use of laboratory animals and were approved by the Institutional Animal Care and Use Committee of Fudan University.

Statistical analysis

Values represent the mean ± SD. Differences were analyzed by *t*-tests. A *P* value ≤0.05 was considered statistically significant. All statistical analyses were conducted using GraphPad Prism 6.

Results

Establishment of the colon SRCC organoid line, YQ-173

We obtained SRCC tissue from a 43-year female patient who underwent left hemicolectomy under informed consent, and then we removed normal tissue and isolated tumor cells through digestion. Isolated cells were plated in adherent Matrigel drops and overlaid with different organoid culture media (Figure 1A, Supplementary Table 1, available at *Carcinogenesis* Online). The addition of 10% FBS in ENR medium greatly facilitated the growth of SRCC organoids (Figure 1A). Among the factors usually added in culturing adenocarcinoma organoids, SB202190, Gastrin, PGE2 and A83-01 did not improve the growth of SRCC, while the addition of NICO obviously inhibited SRCC growth (Figure 1B). Thus, ENR plus 10% FBS without any other factors was set as the optimal culture medium for SRCC.

During culturing, a large number of mucinous cell aggregates were first observed, and scattered cells could be seen in the mucous pool (Supplementary Figure 2A, B, available at *Carcinogenesis* Online). After 2 weeks of culture, cell aggregates became larger and typical signet-ring cells could be seen (Supplementary Figure 2C, available at *Carcinogenesis* Online). A time course of SRCC organoid formation from single signet-ring cell was documented (Figure 1C) with a doubling time of approximately 48 h. The organoid line has been growing in culture for over 18 months with high end stage proliferation, and the line can be frozen, banked and thawed for successful regrowth. After the following characterization of the organoid line, the organoid line was named YQ-173.

Next, we transferred the actively replicating 3D-cultured YQ-173 organoids to a standard culture flask to establish 2D-cultured cells that can be easily handled and to save culture costs. The 2D culture medium was the same as that used for organoids (ENR plus 10% FBS). Signet-ring cells were round and floated freely, and grew exponentially (Supplementary Figure 2D, available at *Carcinogenesis* Online).

Morphology assessment and characterization of YQ-173

Hematoxylin and eosin staining of the original primary tumor showed typical signet-ring cells with a round shape and crescent nuclei (Figure 2A). IF staining of both epithelial cell adhesion molecule (EpCAM) and Mucin 2 indicated epithelial cells with eccentric nuclei pushed by intracellular mucins (Figure 2A). The cultured cells in both 2D and 3D systems exhibited consistent features of the original tumor (Figure 2A, B).

In addition to histological conservation, a representative *in vivo* model should retain expression of the most important and prevalent biomarkers (Figure 2A). Ki-67 reflects the proliferation of cells and Ki-67 was detected in over 90% of cells in both the tumor tissue and organoid. β-catenin and c-Myc reflect the status of the Wnt pathway which is the most important signaling pathway activated in colorectal cancer. Nuclear stainings of both β-catenin and c-Myc were detected in both the tumor tissue and the organoid, indicating that the Wnt pathway was also activated in this case of SRCC, and it was consistent with the fact that the culture of YQ-173 was devoid of WNT-3A. OLFM4 is a stem cell marker, and was consistently negative in both the tumor tissue and the organoid, indicating a distinct origin of SRCC.

To further confirm the biological characteristics of cultured cells, qRT-PCR of goblet-like signature genes, MUC2 and TFF3 (13), was performed. The expression levels of both MUC2 and TFF3 were extremely higher in the SRCC organoids (YQ-173) than those in the normal colon epithelial cell line, NCM460, and the colon adenocarcinoma cell lines, RKO, Caco-2 and LoVo (Figure 2C). MUC2 and TFF3 expression levels were also significantly higher in SRCC tumor tissue than in the normal tissue (Figure 2D), which is consistent with our results in cells.

Electron microscopy findings and chromosome analysis

Ultrastructural examination demonstrated round or semiround nuclei located on one side of the cell. The presence of desmosomes confirmed the epithelial nature of YQ-173 cells and well-developed endoplasmic reticula and Golgi complexes indicated a high protein synthesis workload. Numerous mucus granules filled the cytoplasm. The plasma membrane had numerous straight microvilli (Supplementary Figure 3, available at *Carcinogenesis* Online). All of the above ultrastructures confirmed that YQ-173 cells are signet ring cells. Furthermore, chromosome analysis showed that YQ-173 cells were aneuploid with a median chromosome number of 81 and the structure was considerably aberrant (Supplementary Figure 4, available at *Carcinogenesis* Online), which was in line with the genetic characteristics of malignant tumors.

Tumor formation in athymic nude mice

Approximately 2 weeks after inoculation of the 2D-cultured cells, tumor nodules gradually developed and reached approximately 1000 mm^3 at 6 weeks after injection (Figure 3A, B). The tumor formation rate was 100%. The mice were then killed, and the tumors were excised for morphological study. Histological examination confirmed the presence of signet-ring cells (Figure 3C) and IF staining showed typical epithelial cells with eccentric nuclei and full of intracellular mucin (Figure 3D), which was similar to the original tumor.

RNA seq of YQ-173 organoid

To identify the gene expression signature of SRCC, we performed RNA-seq with YQ-173 organoids. The gene expression pattern of SRCC was different from normal tissue (Figure 4A). Four mucin genes, MUC17, MUC2, MUC5AC and MUC6 were highly expressed in YQ-173 organoids, which might be responsible for the increased production of mucin proteins (Figure 4B). Gene Set Enrichment Analysis found that downregulated genes were enriched in pathways involved in traditional tumorigenesis pathways including epithelial mesenchymal transition and Kirsten rat sarcoma viral oncogene homolog (KRAS) signaling, while upregulated genes in SRCC were mainly enriched in pathways involved in MYC, E2F and MTORC1 targets (Figure 4C). KEGG pathway enrichment analysis indicated that differentially expressed genes in YQ-173 and normal tissue were enriched in

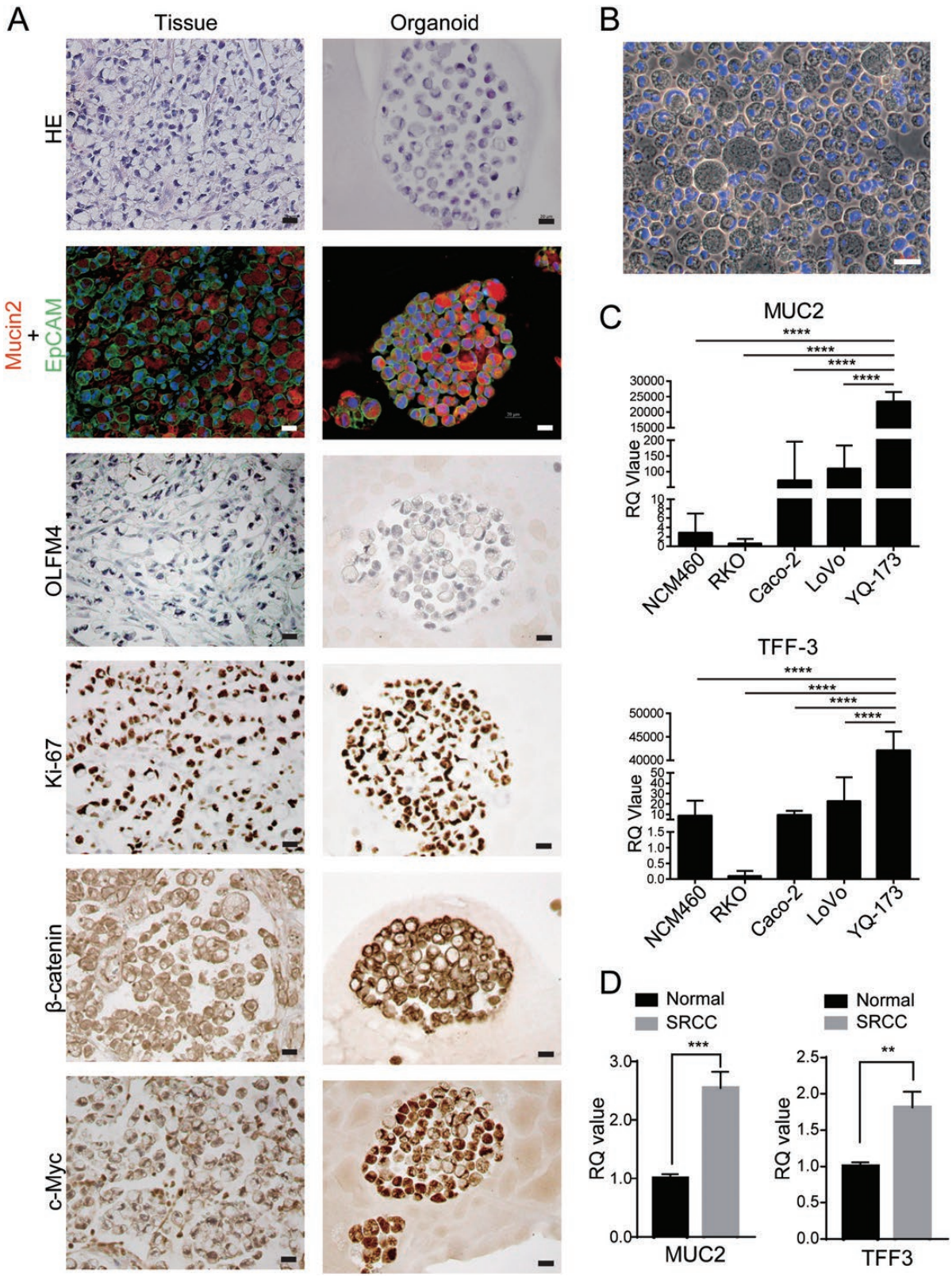

Figure 2. Histology and characterization of the colon SRCC organoid line. (A) Comparative histological, IF and IHC images of colon SRCC (left column) and derived organoid line (right column). Scale bar, 20 μm. (B) Representative image of the 2D-cultured YQ-173 merged with 4′,6-diamidino-2-phenylindole. (C) qRT-PCR results of MUC2 and TFF3 expression levels in YQ-173 compared with NCM460, RKO, Caco-2 and LoVo. (D) qRT-PCR results of MUC2 and TFF3 expression levels in the SRCC tumor tissue compared with the corresponding normal tissue.

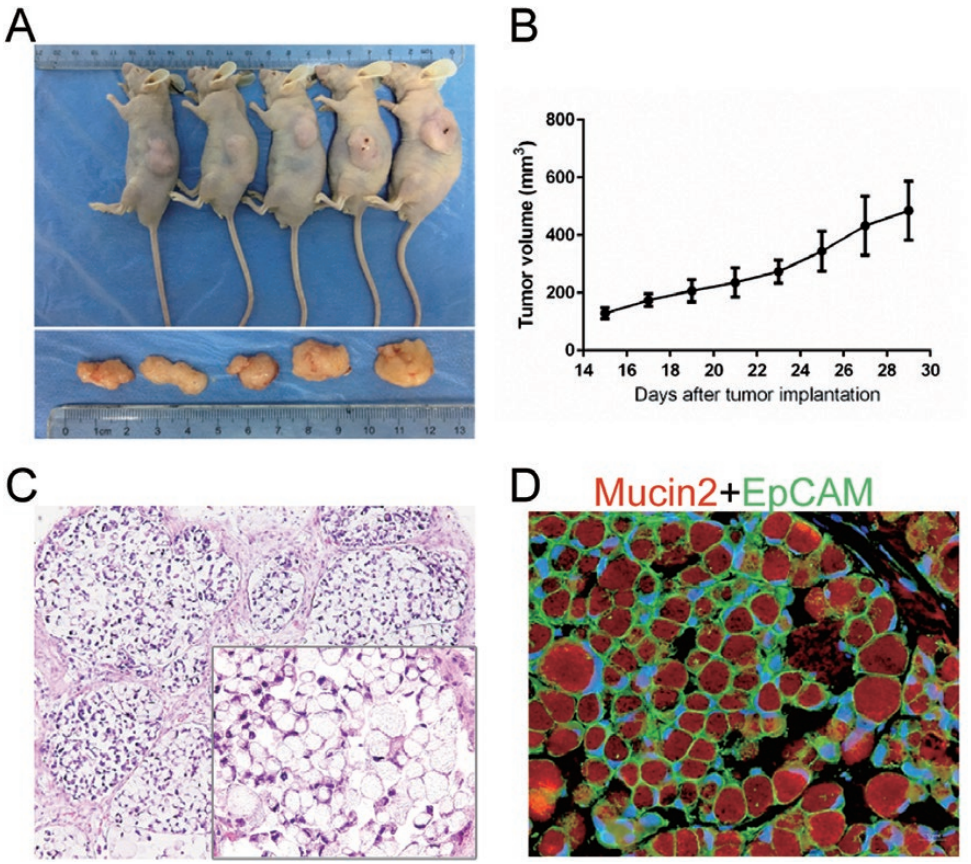

Figure 3. Tumorigenesis of the SRCC organoids *in vivo*. (A) Appearance of the SRCC organoid tumors in five nude mice. SRCC organoids formed tumors in 100% of mice (5/5). (B) Tumor growth curve of organoid xenografts after subcutaneous injection (n = 5). (C) Histological assessment of the formed tumor indicated its SRCC nature. Scale bar, 100 μm. (D) IF and IHC images of Mucin 2 (red) and EpCAM (green) staining of formed tumor. Scale bar, 20 μm.

pathways including in cell adhesion and extracellular matrix–receptor interaction (Figure 4D).

Genomic characterization of YQ-173 organoid

We next employed capture-based targeted DNA sequencing to characterize YQ-173 organoid genomes, including somatic copy number alterations and somatic mutations. To remove germline mutations and compare the concordance of genome profiles, we sequenced genomic DNA isolated from normal tissue, tumor tissue and organoids. Somatic mutations of 10 genes were identified in both tumor tissue and organoids, including driver genes such as FBXW7, KRAS, erb-b2 receptor tyrosine kinase 3 (ERBB3) and PIK3R1, which can activate both WNT and receptor tyrosine kinase (RTK)/Ras pathways (Figure 4E, Supplementary Table 3, available at *Carcinogenesis* Online). Notably, somatic mutation of JAK2 was also detected in both the tumor tissue and organoids, indicating a potential treatment target for this patient. Another 55 genes were detected as mutated in the organoids. No SCNAs were found in the tumor tissue while only focal amplification of mesenchymal to epithelial transition factor (MET) was detected in the organoids (Figure 4F, Supplementary Table 4, available at *Carcinogenesis* Online).

Drug screening

To indentify the possible sensitive drugs or inhibitors for the established line of SRCC, a bespoke 88 compound library targeting 6 main signaling pathways was assembled for screening (Supplementary Table 5, available at *Carcinogenesis* Online). Organoid cultures were mechanically split and plated on 96-well plates. Organoids were allowed to grow for 3 days before being treated with drugs at a concentration of 10 μM and cultured for 5 days before measuring cell viability by Cell Counting Kit-8. Among drugs reaching an inhibitory rate of 50%, 14 targeted the Janus kinase/signal transducers and activators of transcription (JAK/STAT) pathway and 10 of them were JAK2 inhibitors (Supplementary Figure 5, available at *Carcinogenesis* Online). Combining the somatic mutation of JAK2 in both the tumor tissue and YQ-173 organoids, we propose that JAK2 is a potential target to treat this individual patient.

To further clarify the sensitivity to JAK2 inhibitors, two drugs in ongoing clinical trials, AT9283 and Pacritinib, were chosen for further validation, compared with traditional drugs in clinical use, 5-FU and CPT11. Six concentrations of each drug were added and drug sensitivity was represented by the half-maximal inhibitory concentration value. The half-maximal inhibitory concentration values of the YQ-173 organoids to 5-FU, CPT11, AT9283 and Pacritinib were 3.149 μM, 2.642 μM, 0.068 μM and 1.655 μM, respectively (Figure 5A–D). AT9283 was the most effective drug.

Drug response to AT9283 *in vivo*

We then examined the *in vivo* efficacy of AT9283 by using a YQ-173 xenograft mouse model. Once tumors grew larger than 100 mm^3, the mice (n = 6) in vehicle and AT9283 groups were treated with 20 mg/kg i.p. qd, 5 days a week, for 3 weeks. Tumors in the AT9283 group was inhibited significantly compared with

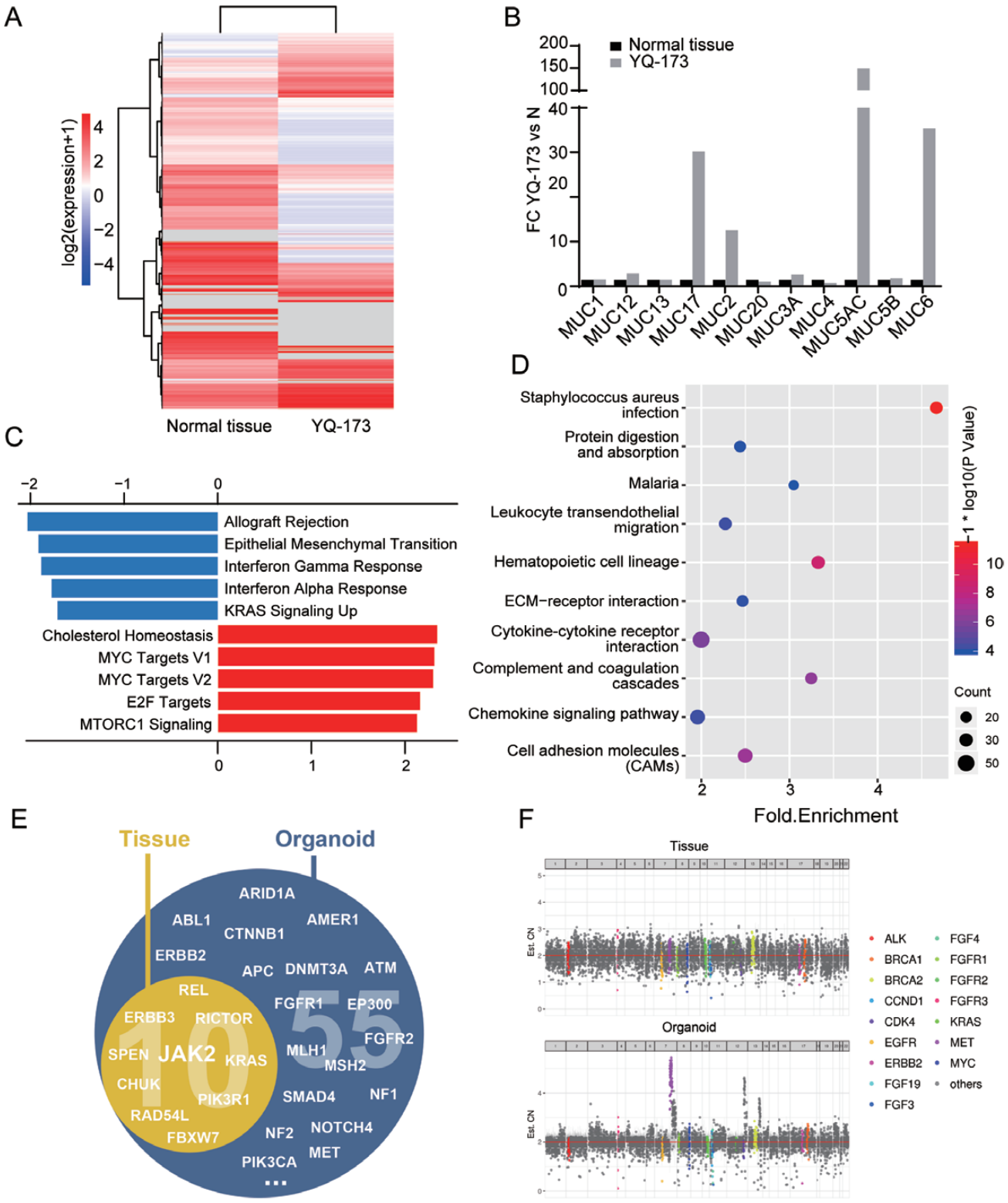

Figure 4. The expression and genomic alterations found in the organoids and the corresponding biopsies. (A) The heatmap showing differentially expressed genes in the SRCC organoids and the corresponding normal tissue. (B) Expression levels of mucin genes in the SRCC organoids and the corresponding normal tissue. (C) GSEA of cancer hallmark signatures enriched in upregulated and downregulated genes between the SRCC organoids and the normal tissue. (D) KEGG pathways enriched in differentially expressed genes between the SRCC organoids and the normal tissue. (E) Concordance of somatic mutations detected in the organoids and the corresponding biopsies. Representative genes are listed. See also Supplementary Table 3, available at *Carcinogenesis* Online. (F) Somatic copy number alterations in the organoids and the corresponding biopsies. Only focal amplification of MET was detected in organoids. See also Supplementary Table 4, available at *Carcinogenesis* Online.

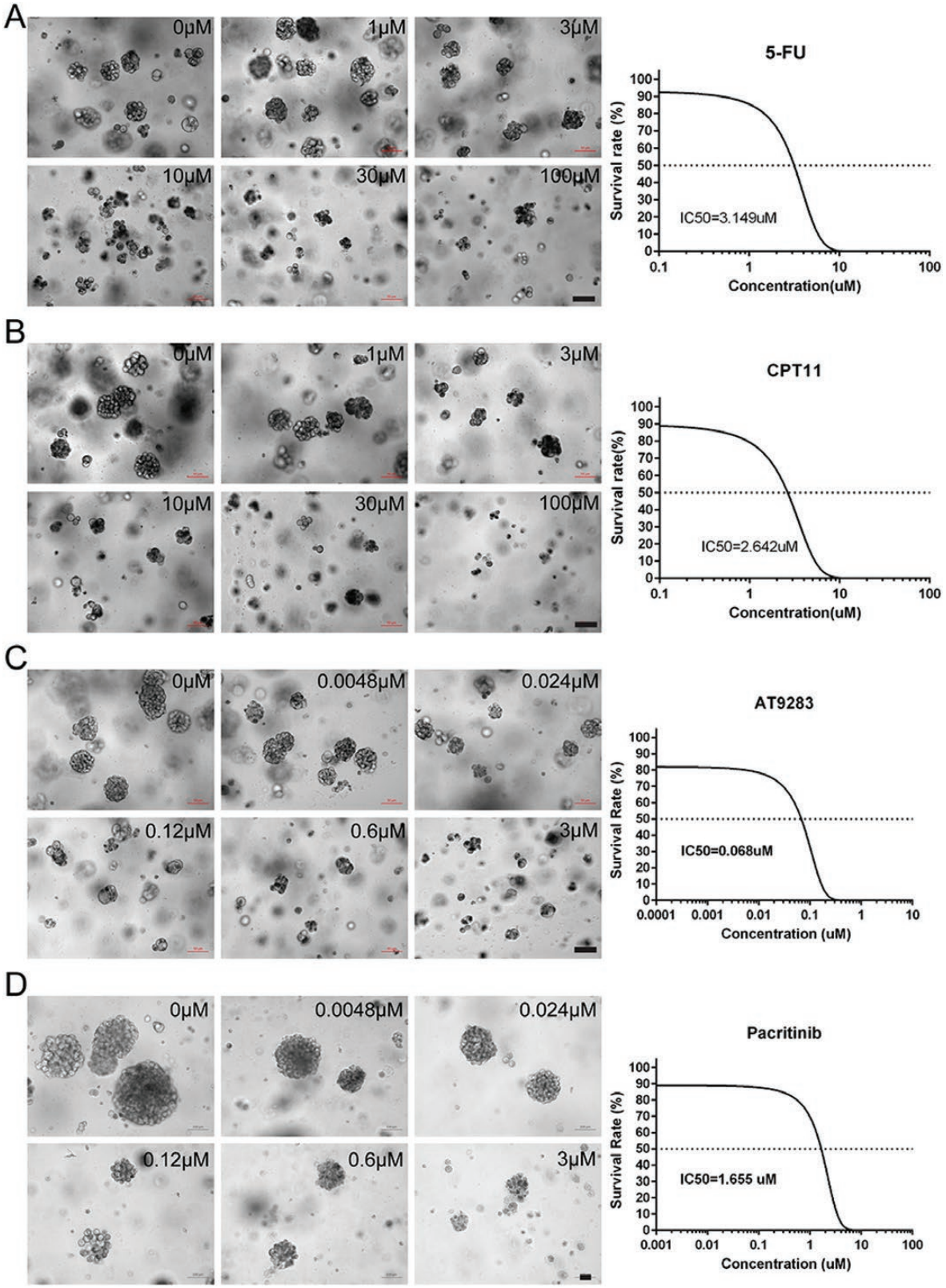

Figure 5. *In vitro* validation of the inhibitory effects of selected drugs on the organoids. (A) Representative images and dose–response curves of the organoids treated with 5-FU. (B) Representative images and dose–response curves of the organoids treated with CPT11. (C) Representative images and dose–response curves of the organoids treated with AT9283. (D) Representative images and dose–response curves of the organoids treated with Pacritinib.

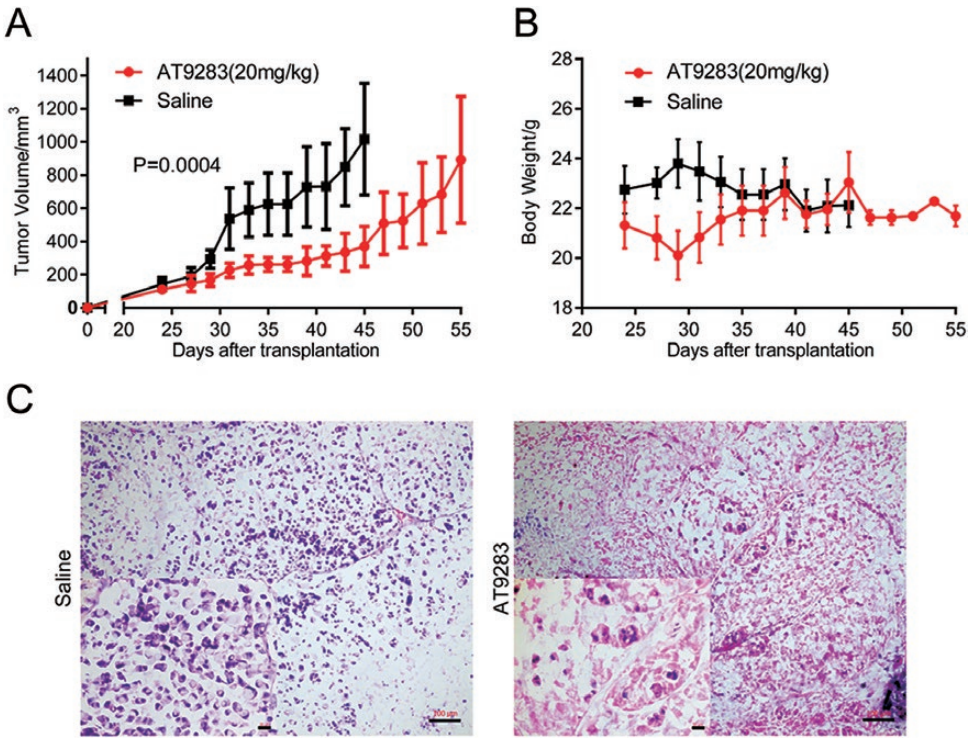

Figure 6. *In vivo* efficacy of AT9283 in the organoid xenografts. (A) Tumor growth curve of the organoid xenografts treated with vehicle (saline) and AT9283 (20 mg/kg) by the intraperitoneal route once daily for 5 days followed by a 2-day break for 3 cycles. Error bars indicate SEs. $n = 6$. (B) Weight change curves of the mice treated with vehicle (saline) and AT9283 (20 mg/kg). Error bars indicate SEs. $n = 6$. (C) Histological assessment of the organoid xenografts treated with vehicle (saline) and AT9283 (20 mg/kg). The tumors treated with AT9283 showed great reduction of signet-ring cells and increase in the mucous pool. Scale bar, 100 μm.

the controls ($P = 0.004$, Figure 6A). Importantly, treatment with the AT9283 did not affect the body weight of the animals (Figure 6B). The mice were killed when the tumor reached 1000 mm^3, and the tumors were excised for morphological study. Histological examination showed a substantial reduction of signet-ring cells and an increase in the mucous pool in tumors treated with AT9283 (Figure 6C).

Discussion

SRCC is a rare subtype of adenocarcinoma with completely distinct biological behavior. 90% of SRCCs occur in the stomach, and colorectal SRCCs account for only 1% of all colorectal cancers. Previous mechanism studies on SRCC were mainly based on gastric cancer cell lines, such as HSC-392 (14), KATOIII (15), NUGC44 (16) and related derivatives. To our knowledge, there is no report of a colorectal SRCC cell line. In the present study, we successfully established and verified the first colon signet ring cell organoid line, YQ-173, and tried to guide a preclinical personalized treatment strategy based on drug screening and capture-based targeted DNA sequencing.

Signet-ring cells are a difficult type of cells to directly culture as 2D cell lines, mainly for the following reasons: (i) signet ring cells interact actively with stroma, while the rapid growth of interstitial cells makes it difficult to separate fibroblasts and cancer cells; (ii) signet-ring cells have a relatively long static period before rapid proliferation, and the improper culture will lead to cell death and (iii) although cell lines can be established from xenografts of tumor tissues, previous reports showed that signet ring cells are difficult to form tumor subcutaneously in the nude mice (15). To solve the above problems, a 3D organoid culture system may be the optimal method to culture signet ring cells *in vitro*. The 3D-culture system is devoid of mesenchymal cells and can help separate the fibroblasts that adhered to the wall (17). In addition, the system can maximally mimic the primary 3D structure of the tumor, so cells can maintain vitality during the static period (7). As described before (18), for primary cells that struggle to survive in long-term planar culture, 2D cells can be derived from 3D organoids, which provide unlimited cell resources. In our study, the SRCC organoid line YQ-173 was successfully established and presented as 'grape-like' cell aggregates. The signet-ring cells were highly purified and devoid of fibroblasts in the optimal culture medium identified. The 2D-cultured SRCC cell lines were then established based on the robust cells and the optimized medium. Although 2D-cultured cells could expand rapidly, they could accumulate mutations and become homogenous through passages (19,20). Therefore, only 2D-cultured YQ-173 cells banked before Passage 10 were used for experiments.

Next, we validated that YQ-173 possesses the characteristics of signet-ring cells by various methods. First, YQ-173 are epithelial cells. The positive expression of EpCAM in the IF staining of organoids and the microvilli and desmosome observed under electron microscopy in 2D-culture cells indicated its epithelial nature. Second, YQ-173 organoids are malignant. The cells had the ability to proliferate rapidly *in vivo* with a cell doubling time of approximately 48 h, and the cells had the ability to promote tumorigenesis in nude mice *in vivo*. Chromosome karyotype evaluation of 2D-cultured cells also showed that the number of chromosomes and structure were greatly aberrated, which was in line with the genetic characteristics of malignant tumors. Third, YQ-173 organoids are mucinous. A large amount of Mucin 2 was positively stained in the cytoplasm of YQ-173 organoids and the nuclei were pushed to the side of the cell.

A large number of mucous particles in the cytoplasm could be observed under the electron microscope, and the endoplasmic reticulum and Golgi bodies were also developed, indicating a high protein synthesis workload. In addition, RNA-seq analysis indicated that the mucin genes were highly expressed in YQ-173 organoids, including MUC2 and MUC5AC, which were verified to be highly expressed in SRCC (21,22), further proving its mucinous nature.

In our study, genomic DNA was also isolated from tumor and organoid culture as well as from normal tissue for deep sequencing of 295 targeted cancer-related genes. Somatic nonsynonymous mutation of 10 genes was detected in both the tumor tissue and organoids. Among these 10 common genes, the inactivating alteration to tumor suppresser FBXW7 activates the WNT pathway, which is consistent with the positive nuclear staining of β-catenin and c-Myc in both the tumor tissue and organoid; activating mutations in KRAS (codon 13) and ERBB3 (codon 104) activates RTK/Ras signaling, which is consistent of the high amplification of Ki-67. Previous studies showed that genomic profiles of organoids derived from primary or metastatic sites were highly concordant with the corresponding biopsy specimen (23,24). In our study, although all mutations of the tumor tissue maintained in organoid culture, 55 novel mutations were detected in organoids, including APC, CTNNB1 and AMER1 in the WNT pathway, ERBB2, MET (also focal amplification), FGFR1/2 and PIK3CA in the RTK/Ras pathway and SMAD family member 4 (SMAD4) in the transforming growth factor-β pathway. The different mutations between the tumor tissue and organoids can be explained by the following reasons. First, the variable time required for the generation of organoid lines in culture may lead to *in vitro* selection of specific tumor clones (25,26). The large number of growth factors added to the organoid media may lead to epigenetic changes and clonal selection. Second, the organoids had high neoplastic purity and the primary tumor specimens had insufficient purity to reveal mutations, especially for such a rare subtype of colorectal cancer, which is full of mucin. To prove this point, the cordant mutations had a mean allelic frequency of 2.82% and 46.41% for the biopsy and organoid, respectively, which could represent an enrichment of a subclonal population in the organoid culture present within the original tumor. Third, colorectal cancer is a type of cancer presenting as microsatellite instable-high in 15% cases and mucinous colorectal cancers have higher proportion of microsatellite instable-high tumors (27). MSI-H tumors tend to acquire novel mutations. Mutations of genes in DNA mismatch repair-associated pathways, mutL homolog 1 (MLH1) and mutS homolog 2 (MSH2), were detected in the organoids, which may have led to the accumulated mutations during propagation.

The organoid culture platform has been validated as a reliable technique for high-throughput drug screening in patient-derived samples (24,28,29). By connecting genetic data, organoids could be an ideal model for screening clinical and preclinical compounds for individualized treatment. It could be of more value for rare types of cancer, which lack a consensus on optimal treatment. In the present study, we detected a mutation of JAK2 in both the biopsy and the organoids of colon SRCC and find a possible effective targeted drug, AT9283, through drug screening. The inhibitory effect of AT9283 on the growth of YQ-173 was validated *in vitro* and *in vivo*, indicating that this preclinical drug could be a treatment choice for this individual patient.

In summary, we successfully established and characterized the first organoid line of colon SRCC, YQ-173, providing an *in vitro* research model for this rare cancer. By combining genomic sequencing and drug screening, we found an effective drug, AT9283, targeting JAK2, which sets an example for organoid-based personalized medicine for rare cancer.

Supplementary material

Supplementary data are available at *Carcinogenesis* online.

Acknowledgements

This work was supported by National Natural Science Foundation of China (31470826, 31670858 and 81672374 to G. H.) and Science and Technology Commission of Shanghai Municipality (16411966300, 18401933402 to J. P. and Shanghai Sailing Program 19YF1409500 to Y. L.). The sponsors have no involvement in study design, in collection, analysis and interpretation of data, in the writing of the report, or in the decision to submit the paper for publication.

Conflict of Interest Statement: The authors declare no potential conflicts of interest.

References

1. Bosman, F.T. *et al.* (2010) *WHO Classification of Tumours of the Digestive System*. 4th edn. World Health Organization, International Agency for Research on Cancer, Geneva, Switzerland.
2. Chew, M.H. *et al.* (2010) Critical analysis of mucin and signet ring cell as prognostic factors in an Asian population of 2,764 sporadic colorectal cancers. *Int. J. Colorectal Dis.*, 25, 1221–1229.
3. Hyngstrom, J.R. *et al.* (2012) Clinicopathology and outcomes for mucinous and signet ring colorectal adenocarcinoma: analysis from the National Cancer Data Base. *Ann. Surg. Oncol.*, 19, 2814–2821.
4. Nitsche, U. *et al.* (2013) Mucinous and signet-ring cell colorectal cancers differ from classical adenocarcinomas in tumor biology and prognosis. *Ann. Surg.*, 258, 775–782; discussion 782.
5. Wang, R. *et al.* (2016) The characteristics and prognostic effect of E-cadherin expression in colorectal signet ring cell carcinoma. *PLoS One*, 11, e0160527.
6. Lancaster, M.A. *et al.* (2014) Organogenesis in a dish: modeling development and disease using organoid technologies. *Science*, 345, 1247125.
7. Clevers, H. (2016) Modeling development and disease with organoids. *Cell*, 165, 1586–1597.
8. Sato, T. *et al.* (2011) Long-term expansion of epithelial organoids from human colon, adenoma, adenocarcinoma, and Barrett's epithelium. *Gastroenterology*, 141, 1762–1772.
9. Rotolo, J.A. *et al.* (2008) Bax and Bak do not exhibit functional redundancy in mediating radiation-induced endothelial apoptosis in the intestinal mucosa. *Int. J. Radiat. Oncol. Biol. Phys.*, 70, 804–815.
10. Hua, G. *et al.* (2012) Crypt base columnar stem cells in small intestines of mice are radioresistant. *Gastroenterology*, 143, 1266–1276.
11. Chen, H. *et al.* (2010) The role of nucleophosmin/B23 in radiation-induced chromosomal instability in human lymphoblastoid cells of different p53 genotypes. *Int. J. Radiat. Biol.*, 86, 1031–1043.
12. Tomayko, M.M. *et al.* (1989) Determination of subcutaneous tumor size in athymic (nude) mice. *Cancer Chemother. Pharmacol.*, 24, 148–154.
13. Sadanandam, A. *et al.* (2013) A colorectal cancer classification system that associates cellular phenotype and responses to therapy. *Nat. Med.*, 19, 619–625.
14. Yanagihara, K. *et al.* (1991) Establishment and characterization of human signet ring cell gastric carcinoma cell lines with amplification of the c-myc oncogene. *Cancer Res.*, 51, 381–386.
15. Sekiguchi, M. *et al.* (1978) Establishment of cultured cell lines derived from a human gastric carcinoma. *Jpn. J. Exp. Med.*, 48, 61–68.
16. Fukui, Y. *et al.* (1989) Detection of glycoproteins as tumor-associated Hanganutziu-Deicher antigen in human gastric cancer cell line, NUGC4. *Biochem. Biophys. Res. Commun.*, 160, 1149–1154.

17. Fujii, M. *et al.* (2016) A colorectal tumor organoid library demonstrates progressive loss of niche factor requirements during tumorigenesis. *Cell Stem Cell*, 18, 827–838.
18. Schlaermann, P. *et al.* (2016) A novel human gastric primary cell culture system for modelling Helicobacter pylori infection *in vitro*. *Gut*, 65, 202–213.
19. Sachs, N. *et al.* (2014) Organoid cultures for the analysis of cancer phenotypes. *Curr. Opin. Genet. Dev.*, 24, 68–73.
20. Byrne, A.T. *et al.* (2017) Interrogating open issues in cancer precision medicine with patient-derived xenografts. *Nat. Rev. Cancer*, 17, 254–268.
21. Fujimoto, A. *et al.* (2017) Differences between gastric signet-ring cell carcinoma and poorly differentiated adenocarcinoma: a comparison of histopathologic features determined by mucin core protein and trefoil factor family peptide immunohistochemistry. *Pathol. Int.*, 67, 398–403.
22. Terada, T. (2013) An immunohistochemical study of primary signet-ring cell carcinoma of the stomach and colorectum: II. Expression of MUC1, MUC2, MUC5AC, and MUC6 in normal mucosa and in 42 cases. *Int. J. Clin. Exp. Pathol.*, 6, 613–621.
23. Weeber, F. *et al.* (2015) Preserved genetic diversity in organoids cultured from biopsies of human colorectal cancer metastases. *Proc. Natl. Acad. Sci. USA*, 112, 13308–13311.
24. van de Wetering, M. *et al.* (2015) Prospective derivation of a living organoid biobank of colorectal cancer patients. *Cell*, 161, 933–945.
25. Gao, D. *et al.* (2014) Organoid cultures derived from patients with advanced prostate cancer. *Cell*, 159, 176–187.
26. Boj, S.F. *et al.* (2015) Organoid models of human and mouse ductal pancreatic cancer. *Cell*, 160, 324–338.
27. Andrici, J. *et al.* (2016) Mismatch repair deficiency as a prognostic factor in mucinous colorectal cancer. *Mod. Pathol.*, 29, 266–274.
28. Vlachogiannis, G. *et al.* (2018) Patient-derived organoids model treatment response of metastatic gastrointestinal cancers. *Science*, 359, 920–926.
29. Sachs, N. *et al.* (2018) A living biobank of breast cancer organoids captures disease heterogeneity. *Cell*, 172, 373–386.e10.